Tracer particles and seeding for particle image velocimetry

1997 Meas. Sci. Technol. 8 1406

(http://iopscience.iop.org/0957-0233/8/12/005)

Meas. Sci. Technol. **8** (1997) 1406–1416. Printed in the UK PII: S0957-0233(97)84480-3

Tracer particles and seeding for particle image velocimetry

A Melling

Lehrstuhl für Strömungsmechanik, Universität Erlangen-Nürnberg, Cauerstrasse 4, D-91058 Erlangen, Germany

Received 28 May 1997, accepted for publication 2 October 1997

Abstract. The size specifications for suitable tracer particles for particle image velocimetry (PIV), particularly with respect to their flow tracking capability, are discussed and quantified for several examples. A review of a wide variety of tracer materials used in recent PIV experiments in liquids and gases indicates that appropriately sized particles have normally been used. With emphasis on gas flows, methods of generating seeding particles and for introducing the particles into the flow are described and their advantages are discussed.

1. Introduction

During the last decade, the technique of particle image velocimetry (PIV, reviewed recently by Grant (1997)) has seen rapidly increasing application for non-intrusive diagnostic investigations of complex flow fields, both on its own and as a complement to laser Doppler anemometry (LDA). Both methods rely on scattering particles suspended in the flow to provide the velocity information for the continuous medium (liquid or gas). The accuracy of the velocity field determination is ultimately limited by the ability of the scattering particles to follow the instantaneous motion of the continuous phase. A compromise between reducing the particle size to improve flow tracking and increasing the particle size to improve light scattering is, therefore, necessary (Melling and Whitelaw 1973).

Proper flow seeding is particularly critical with PIV. Even when using high laser pulse energies, the distribution of this energy over a laser sheet leads to an energy density which is low relative to that typical in LDA. Furthermore, to secure sufficient detail in the flow field a higher spatial concentration of particles is generally needed than with LDA, with which it is possible (within limitations imposed by flow unsteadiness, biased sampling of the velocity statistics or running costs) to wait indefinitely for the arrival of a scattering particle in the probe volume. There is also less scope in PIV for adjusting the position of the seeding source to optimize the data rate, so particle generators producing ample seeding are necessary. A uniform seeding size is desirable in order to avoid excessive intensity from larger particles and background noise, decreasing the accuracy, from small particles.

In the following sections, this paper will consider the specifications for PIV seeding particles with respect to light scattering characteristics (section 2) and the aerodynamic tracking capability (section 3). A review of the types of particle used in various PIV applications is given in section 4 and methods of generating and seeding suitable particles are described in section 5.

Table 1. The scattering cross section as a function of the particle size.

Diameter d_p	Scattering cross section C_s	
Molecule		$\simeq 10^{-33}$ m^2
1 μm	$C_s \simeq (d_p/\lambda)^4$	$\simeq 10^{-12}$ m^2
10 μm	$C_s \simeq (d_p/\lambda)^2$	$\simeq 10^{-9}$ m^2

2. Scattering characteristics of particles

The choice of optimal diameter for seeding particles is a compromise between an adequate tracer response of the particles in the fluid, requiring small diameters, and a high signal-to-noise ratio (SNR) of the scattered light signal, necessitating large diameters. For the objectives of this paper, the tracking capability of the seeding particles is of greater concern, but light scattering characteristics of particles are considered briefly in this section.

A convenient measure of the (spatially integrated) light scattering capability is the scattering cross section C_s, defined as the ratio of the total scattered power P_s to the laser intensity I_0 incident on the particle:

$$C_s = P_s / I_0. \tag{1}$$

Figure 1 shows the variation of C_s as a function of the ratio of the particle diameter d_p to the laser wavelength λ for spherical particles with a refractive index $m = 1.6$. Table 1 compares approximate values for a diatomic molecule such as nitrogen or oxygen and two larger particles.

These examples indicate clearly the enormous difference between the light scattering cross sections of molecules and those of particles of diameter 1–10 μm

0957-0233/97/121406+11$19.50

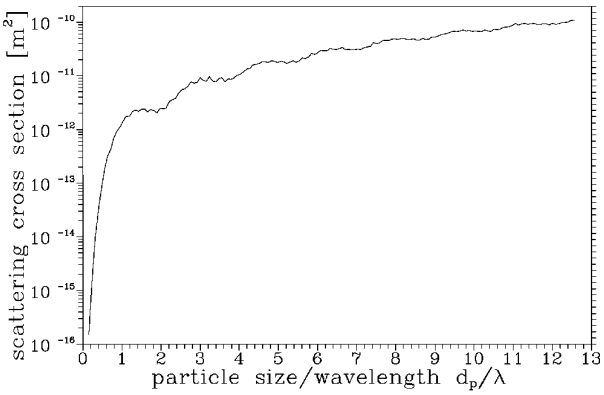

Figure 1. The scattering cross section as a function of the particle size (refractive index $m = 1.6$).

which, as will be seen in section 4, are typical seeds for PIV experiments. Elastic (Rayleigh) scattering from molecules is far too weak for PIV even with illumination by a laser of maximum available power or pulse energy. In terms of SNR, of course, PIV applications are confronted with lower incident light intensity compared with LDA, consequent on spreading the laser energy spatially over a light sheet. The detector efficiency is also an important factor in determining the SNR.

In PIV experiments one normally observes light scattered at 90° from the incident light sheet, so not only the angular distribution of the scattered light intensity from seeding particles is of interest but also the overall scattering cross section. Studies of scattering from spherical particles, such as those conducted for laser Doppler anemometry, have shown that the intensity ratio I_{s90}/I_{s0} of 90° scattered light to forward scattered light is a strong function both of the size parameter d_p/λ and of the refractive index m. The angular distribution of scattered light in the vicinity of 90° is complex, with several nodes whose exact positions are strongly size dependent (Durst *et al* 1981 p 60). Spatial averaging over a finite aperture of the collecting optics will, however, tend to reduce the influence of these fluctuations. In broad terms, therefore, the ratio I_{s90}/I_{s0} decreases with increasing value of the size parameter d_p/λ, with values roughly in the range 10^{-1}–10^{-3} for scattering particles useful in PIV. The resulting intensity of the scattered light for a given light sheet intensity will depend on the combined influences of C_s and I_{s90}/I_{s0}, which exhibit opposing tendencies with increasing particle size. In general, larger particles will still give stronger signals. For further details regarding scattering characteristics of particles suitable for PIV, reference is made to the paper of Mengel and Mørck (1993).

3. Tracking characteristics of particles

3.1. The equation of particle motion

In this section an analysis of the motion of suspended particles in a continuous medium is applied to the specification of the maximum size of tracking particles for two examples, turbulent flows and transonic flows.

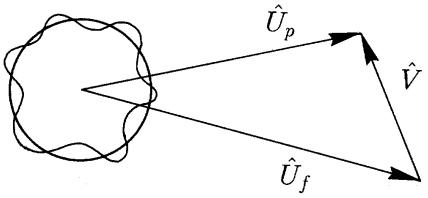

Figure 2. The relative motion of a suspended particle.

Attention is directed mainly to gas flows, for which the choice of particle size is normally more critical than it is in liquids.

If external forces (gravitational, centrifugal and electrostatic) can be considered negligible, the tracking capability of suspended particles is influenced only by the particle shape, particle diameter d_p, particle density ρ_p, fluid density ρ_f and fluid dynamic viscosity μ or kinematic viscosity $\nu = \mu/\rho_f$. Although the shape of a particle significantly affects the flow resistance, only the motion of spherical particles can be analysed. The assumption of spherical form is valid for small droplets and monodisperse solid particles. For irregular particles, it is commonly assumed that they can be treated as spheres with an aerodynamically equivalent diameter.

The particle concentration is assumed to be so low that the particles are suspended in a fluid of infinite extent. This assumption is not restrictive for concentrations (up to about 10^9 m^{-3}) which can be achieved by dispersion of particles in gases. At this concentration, 1 μm particles have an average separation of 1000 diameters.

Equation (2) for unsteady motion (t is time) of a suspended sphere, as given by Basset (1888), relates the instantaneous relative velocity $\hat{V} = \hat{U}_p - \hat{U}_f$ between the particle and the fluid to the instantaneous velocities $\hat{U}_p$ and $\hat{U}_f$ of the particle and the fluid respectively (figure 2).

$$\frac{\pi d_p^3}{6}\rho_p\frac{\mathrm{d}\hat{U}_p}{\mathrm{d}t} = -3\pi\mu d_p\hat{V} + \frac{\pi d_p^3}{6}\rho_f\frac{\mathrm{d}\hat{U}_f}{\mathrm{d}t} - \frac{1}{2}\frac{\pi d_p^3}{6}\rho_f\frac{\mathrm{d}\hat{V}}{\mathrm{d}t} - \frac{3}{2}d_p^2(\pi\mu\rho_f)^{1/2}\int_{t_0}^{t}\frac{\mathrm{d}\hat{V}}{\mathrm{d}\xi}\frac{\mathrm{d}\xi}{(t-\xi)^{1/2}}. \quad (2)$$

The acceleration force and the viscous resistance according to Stokes' law are given in the first two terms. The acceleration of the fluid leads to a pressure gradient in the vicinity of the particle and hence to an additional force given by the third term. The fourth term represents the resistance of an inviscid fluid to the acceleration of the sphere, as given by the potential theory. The first, third and fourth terms combined correspond to the accelerating force on a sphere whose mass is increased by an additional 'virtual' mass equal to half of the fluid mass which is displaced by the sphere. The final term is the 'Basset history integral' which defines the resistance caused by the unsteadiness of the flow field.

Stokes' drag law is considered to apply when the particle Reynolds number Re_p is smaller than about unity:

$$Re_p = \frac{\rho_f\hat{V}d_p}{\mu} = \frac{\hat{V}d_p}{\nu}. \quad (3)$$

This condition holds true for small particles and small relative velocity $\hat{V}$. Stokes' drag law gives a conservative estimate of the tracking ability of particles, since the actual drag tends to be higher (Dring 1982).

Although equation (2) suffices for most flows, in some cases body forces are present which introduce additional effects. One such case is the shear flow in which a transverse lift force is exerted on a suspended particle (Saffman 1965). In swirling flow the centrifugal force which was explicitly neglected in equation (2) is important; this will accelerate a particle radially out of the vortex core (Durst *et al* 1981 p 292). In the practice of seeding flows this effect may, however, cause less concern than the difficulty often encountered in introducing particles into a vortex in the first place (section 5.2.2).

3.2. The motion of particles in turbulent flow

Solutions of equation (2) for particle responses in turbulent flow apply for homogeneous, stationary turbulence (valid for small-scale motions) with particles smaller than the smallest turbulence eddies (which is satisfactory for PIV applications). Furthermore, the immediate surroundings of the particle are supposed always to consist of the same fluid molecules, consistent with there being little relative motion between a particle and the fluid. Under these restrictions, the solution can be expressed either as the relative amplitude η and phase response β of the instantaneous particle and fluid motions (Hjelmfelt and Mockros 1966) or as the ratio $\overline{u_p^2}/\overline{u_f^2}$ of the fluctuation energies of the time-averaged particle and fluid motions (Chao 1964, Haertig 1976). An extensive discussion of equation (2) and its solution for turbulent flow, with attention to the unsteady dynamic forces on a spherical particle at finite Reynolds number, has been given by Mei (1996).

3.2.1. The solution of Hjelmfelt and Mockros. Hjelmfelt and Mockros (1966) expressed $\hat{U}_p$ and $\hat{U}_f$ as Fourier integrals:

$$\hat{U}_f = \int_0^\infty [\zeta \cos(\omega t) + \lambda \sin(\omega t)]\,\mathrm{d}\omega \tag{4}$$

$$\hat{U}_p = \int_0^\infty \eta[\zeta \cos(\omega t + \beta) + \lambda \sin(\omega t + \beta)]\,\mathrm{d}\omega \tag{5}$$

where ω is the angular frequency of the turbulent motion. They then solved for the amplitude ratio η of the particle and fluid velocities and the phase lag β of the particle motion as functions of the density ratio $s = \rho_p/\rho_f$ and the Stokes number Sk, a characteristic non-dimensional frequency of the particle response. Sk is defined here as

$$Sk = \left(\frac{\omega}{\nu}\right)^{1/2} d_p \tag{6}$$

although other definitions are to be found in the literature.

3.2.2. The solution of Chao. Chao (1964) considered the Fourier transform of the equation of motion (2) and derived an energy transfer function $\Omega^{(1)}/\Omega^{(2)}$. Using the notation of the present paper, the functions $\Omega^{(1)}$ and $\Omega^{(2)}$ can be written as

$$\Omega^{(1)} = 1 + f + \frac{f^2}{2} + \frac{f^3}{6} + \frac{f^4}{36} \tag{7}$$

$$\Omega^{(2)} = 1 + f + \frac{f^2}{2} + \left(\frac{2s+1}{3}\right)\frac{f^3}{6} + \left(\frac{2s+1}{3}\right)^2 \frac{f^4}{36} \tag{8}$$

where $f = Sk/\sqrt{2}$. Chao showed that the kinetic energies of the particle velocity fluctuations $\overline{u_p^2}$ and the fluid velocity fluctuations $\overline{u_f^2}$ are related by

$$\frac{\overline{u_p^2}}{\overline{u_f^2}} = \int_0^\infty \frac{\Omega^{(1)}}{\Omega^{(2)}} E(\omega)\,\mathrm{d}\omega \tag{9}$$

where $E(\omega)$ is the energy spectral density function, normalized to an integral of unity over all turbulence frequencies ω. Chao used an energy spectrum corresponding to fully developed turbulent pipe flow at high Reynolds number. When particle and fluid densities are equal, then $s = 1$ and so $\Omega^{(2)} = \Omega^{(1)}$. It then follows from equation (9) that $\overline{u_p^2} = \overline{u_f^2}$; that is, the particles follow the fluid motion exactly. Mei (1996) has applied the concept of the energy transfer function to the instantaneous particle and fluid motion.

3.2.3. Solutions for a high density ratio. For the dynamics of solid particles in liquid flow, the effect of the final (Basset) term in equation (2) need not always be significant, but the third and fourth (pressure gradient and added mass) terms must always be considered. For PIV experiments in gases (in the absence of shear effects and centrifugal forces), however, only the first two terms are important because of the large density ratio $s \gg 1$. The equation of motion (2) can then be greatly simplified:

$$\frac{\mathrm{d}\hat{U}_p}{\mathrm{d}t} = -C(\hat{U}_p - \hat{U}_f) \tag{10}$$

where C is a characteristic frequency of the particle motion, defined in terms of a drag coefficient C_D as

$$C = \frac{3}{4} C_D Re_p \frac{\mu}{\rho_p d_p^2}. \tag{11}$$

For Stokes' resistance $C_D = 24/Re_p$ and

$$C = \frac{18\mu}{\rho_p d_p^2} = \frac{18\omega}{Sk^2 s}. \tag{12}$$

For $s \gg 1$ the solution of Hjelmfelt and Mockros reduces to

$$\eta = \left(1 + \frac{\omega_c^2}{C^2}\right)^{-1/2} \tag{13}$$

$$\tan\beta = -\frac{\omega_c}{C} = -\frac{Sk^2 s}{18} \tag{14}$$

Table 2. Particle response in turbulent flow (η = 0.99).

Particle	ρ_p (kg m^{-3})	Gas (10^5 Pa)	Density ratio s	Viscosity ν (m^2 s^{-1})	f_c (kHz)	Sk_c	d_p (μm)
TiO_2	3500	Air (300 K)	2950	1.50×10^{-5}	1	0.0295	1.44
					10		0.45
Al_2O_3	3970	Flame (1800 K)	20250	3.00×10^{-4}	1	0.0113	2.46
					10		0.78
Glass	2600	Air (300 K)	2190	1.50×10^{-5}	1	0.0342	1.67
					10		0.53
Olive oil	970	Air (220 K)	617	1.45×10^{-5}	1	0.0645	3.09
					10		0.98
Microballoon	100	Air (300 K)	84.5	1.50×10^{-5}	1	0.1742	8.50
					10		2.69

where ω_c is the highest turbulence frequency of interest. A rational quantification of ω_c could be made in terms of the Kolmogorov time scale $\tau = (\nu/\epsilon)^{1/2}$ as a measure of the smallest turbulent eddies. τ depends on the local turbulence dissipation rate ϵ, however, which for most flows of practical interest is not quantifiable with any precision. So ω_c will normally be estimated by experience; depending on the mean velocity, maximum turbulence frequencies lie in the range $f_c = \omega_c/(2\pi) = 10^3$–$10^6$ Hz.

Furthermore, from equations (7), (8) and (12) for large s values

$$\frac{\Omega^{(1)}}{\Omega^{(2)}} = \left(1 + \frac{\omega^2}{C^2}\right)^{-1}. \tag{15}$$

If the energy spectrum for fully developed turbulent pipe flow is approximated as proposed by Haertig (1976):

$$E(\omega) = \frac{2}{\pi\omega_c}\left(1 + \frac{\omega^2}{\omega_c^2}\right)^{-1} \tag{16}$$

where $E(\omega)$ corresponds to the simple autocorrelation function $R(\tau) = \mathrm{e}^{-\omega\tau}$, then an analytical solution is possible by substituting equations (15) and (16) into equation (9) and integrating:

$$\frac{\overline{u_p^2}}{\overline{u_f^2}} = \left(1 + \frac{\omega_c}{C}\right)^{-1}. \tag{17}$$

The curves for various characteristic frequencies C calculated on the basis of equation (17) in figure 3 show the relative fluctuation intensities of the particle and fluid motions $\overline{u_p^2}/\overline{u_f^2}$ in a turbulent flow summed over all turbulence frequencies below f_c. The curve for $C = 1.2 \times 10^5$ s^{-1} corresponds approximately to the motion of a 1 μm water droplet in air. Higher C values lead to better flow tracking behaviour of the particle.

When specifying a maximum seeding particle size, a criterion for acceptable flow tracking has to be chosen. In the limit of a large density ratio, criteria based on η and $\overline{u_p^2}/\overline{u_f^2}$ can be related by eliminating ω_c/C from equations (13) and (17), leading to equivalent limits $\eta = 0.99$ and $\overline{u_p^2}/\overline{u_f^2} = 0.95$. Using this criterion and frequency responses $f_c = 1$ and 10 kHz, limiting particle diameters d_p relevant to PIV experiments in air are given in table 2.

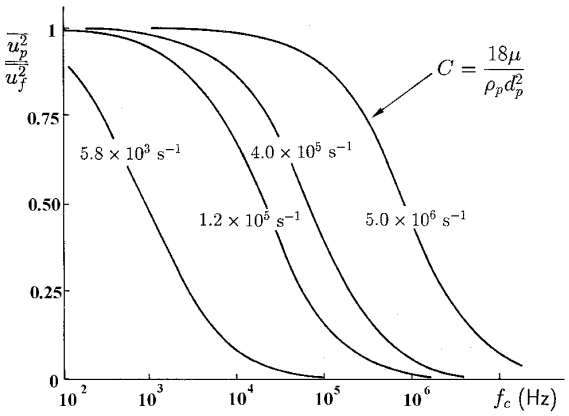

Figure 3. The response of particles in turbulent flow (after Haertig (1976)).

The calculations for a range of seeding materials (selected mainly from table 3) indicate that a diameter up to 2–3 μm is acceptable for a moderate frequency response of 1 kHz. For a better frequency response (10 kHz), however, the diameter should not exceed 1 μm.

The case $s \ll 1$, relevant to the motion of small gas bubbles in liquid, has been considered by Mei (1996), who showed that such particles could move with a greater fluctuation energy than the turbulence energy of the flow. Tracer bubbles, however, have hardly ever been used in PIV experiments; an exception is the work of Dieter *et al* (1994), see table 4.

3.3. The motion of particles in transonic flow

For high speed (transonic and supersonic) flow the motion of an entrained particle of high density ratio s can be represented by equation (10), if a suitable expression for the drag coefficient C_D is inserted. Many semi-empirical expressions for C_D have been proposed in the literature; in addition to a dependence on the Reynolds number Re_p these formulae may include the Mach number based on the relative velocity $\hat{V}$ or the Knudsen number Kn_p, defined in terms of the mean free path l of the gas molecules as $Kn_p = l/d_p$.

Table 3. Seeding particles in gas flows.

Material	d_p (μm)	Laser	Pulse energy, pulse time	Light sheet w (mm)	Light sheet t (mm)	Reference
TiO_2 (m = 2.6, ρ = 3500 kg m^{-3})	<1	Nd:YAG	10 mJ, 20 ns	15	0.3	Reuss *et al* (1989)
TiO_2, ZrO_2	0.7–1	Nd:YAG	110 mJ, 12 ns			Paone *et al* (1996)
Al_2O_3 (m = 1.76,	0.3	Nd:YAG	400 mJ		0.2	Muniz *et al* (1996)
ρ = 3970 kg m^{-3})	3	Nd:YAG	9 mJ, 6 ns			Anderson *et al* (1996)
	0.8	Ruby	20 ns	150	≃1	Krothapalli *et al* (1996)
Polycrystalline	30	Nd:YAG	135 mJ, 6 ns			Grant *et al* (1994)
Glass	30	Ruby	30 mJ, 30 ns			Schmidt and Löffler (1993)
Oil smoke	1	Ruby	5 J			Stewart *et al* (1996)
Corn oil	1–2	Nd:YAG	100 mJ			Jakobsen *et al* (1994)
Oil	1–2	Nd:YAG	120 mJ		0.4	Westerweel *et al* (1993)
Olive oil (m = 1.47, ρ = 970 kg m^{-3})	1.06	Nd:YAG	70 mJ, 16 ns	200	0.5	Höcker and Kompenhans (1991) Fischer (1994) Raffel *et al* (1996)

A situation frequently encountered in transonic flow is the normal or oblique shock; this will be used for the purposes of illustration. For PIV applications the particle's response is conveniently quantified by the relaxation time or the relaxation distance required for the particle velocity lag $|\hat{V}| = |\hat{U}_p - \hat{U}_f|$ after the shock to be reduced by a factor $1/\mathrm{e} = 0.368$. A simple approach (Meyers and Feller 1975, Dring 1982) provides insight into the phenomenon by treating the particle's motion through a shock in a piecewise fashion as a step deceleration. Using equation (10), the relaxation time is simply $1/C$. If the initial particle velocity is $\hat{U}_{pi}$, the solution for the instantaneous particle velocity $\hat{U}_p$ as a function of time t is

$$\left|\frac{\hat{U}_f - \hat{U}_p}{\hat{U}_f - \hat{U}_{pi}}\right| = \mathrm{e}^{-Ct}. \tag{18}$$

In the example of figure 4 for air flow through a 55° oblique shock at an upstream Mach number of 1.5 and a static temperature of 300 K, the approach velocity is 521 m s^{-1}. Across the shock the normal component of the gas velocity changes from 427 to 307 m s^{-1}. From equation (12) the relaxation time for a 1 μm water droplet is 3.70 μs and in that time the particle velocity according to equation (18) decreases to 383 m s^{-1}, corresponding to a lag of 76 m s^{-1} (25%) relative to the air velocity. Clearly, smaller particles would be preferable as PIV tracers.

To determine the two-dimensional particle motion across an oblique shock it is necessary to solve for the velocity components U_{px} and U_{py} in the x and y directions, using modified forms of equation (10) with $j = x, y$:

$$\frac{\mathrm{d}\hat{U}_{pj}}{\mathrm{d}t} = -\frac{3}{4}C_D Re_p \frac{\mu}{\rho_p d_p^2}(\hat{U}_{pj} - \hat{U}_{fj}). \tag{19}$$

The particle trajectory (x_p, y_p) follows by integration from the definitions $\mathrm{d}x_p/\mathrm{d}t = U_{px}$ and $\mathrm{d}y_p/\mathrm{d}t = U_{py}$. In the example of figure 4, equations (19) were solved using a modified Stokes drag in the form

$$C_D = \frac{24}{Re_p(1 + Kn_p)}. \tag{20}$$

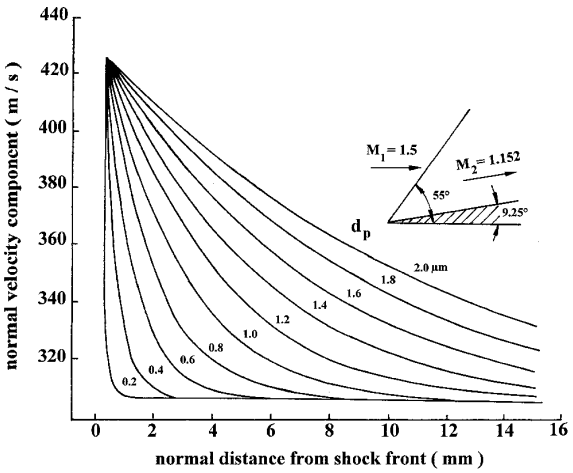

Figure 4. The response of particles downstream of an oblique shock.

The curves show the component of the particle velocity normal to the shock as a function of the normal distance downstream of the shock, for water droplets of given size and density 1000 kg m^{-3}. Only particles smaller than about 0.3 μm recover rapidly after the shock; 1 μm particles, for example, require a distance of about 12 mm in which to decelerate to the gas velocity. In comparison with figure 4 the simple model is quite good for larger particles but gives increasing deviations for smaller particles, attributable to the Knudsen number correction in equation (20). According to the more complete model, after one relaxation time $\tau = 14.8$ μs a 2.0 μm particle attains a velocity of 387 m s^{-1}, but a 0.4 μm particle ($\tau = 0.6$ μs) has decelerated only to 400 m s^{-1}. The simple model gives 383 m s^{-1} in both cases.

Table 4. Seeding particles in liquid flows.

Material	d_p (μm)	Laser	CW power or energy, time	Light sheet w (mm)	Light sheet t (mm)	Reference
TiO_2	3	Nd:YAG				Longmire and Alahyari (1994)
Al_2O_3	9.5	Ruby	2 J, 30 ns	100	0.8	Liu *et al* (1991)
Conifer pollen (ρ = 1000 kg m^{-3})	50–60	Ar ion	1-2 W			Westergaard *et al* (1993) McCluskey *et al* (1995) Gallagher and McEwan (1996)
Polymer (ρ = 1030 kg m^{-3})	30	Ar ion	0.5–5 W		0.5	Draad and Westerweel (1996) McCluskey *et al* (1996)
Phosphorescent polymer	80	Ar ion	5 W		1	Willert and Gharib (1991)
Fluorescent	50	Nd:YAG				Hart (1996)
	20	Cu vapour	45 W		1	Roth *et al* (1995)
Polystyrene	500					Khoo *et al* (1992)
(ρ = 1050 kg m^{-3})	15	Ruby	25 mJ, 20 ns			Zhang *et al* (1996)
Thermoplastic (ρ = 1020 kg m^{-3})	6	Nd:YAG		50	2	Hassan *et al* (1994)
Reflective	60	Ar ion	18 W			Grant *et al* (1992)
(ρ = 1010 kg m^{-3})	30	Ar ion	12–18 W	200		Grant and Wang (1994)
Metallic coated	4	Ar ion	2 W		2	Magness *et al* (1993)
	14	Ar ion			1	Johari *et al* (1996)
Microspheres (ρ = 700 kg m^{-3})	$<$30	Ar ion				Graham and Soria (1994)
H_2 bubbles		Ar ion	1 W		0.3	Dieter *et al* (1994)

4. Seeding particles in PIV applications

For most experiments it is desirable that seeding particles be non-toxic, non-corrosive, non-abrasive, non-volatile and chemically inert. Considering these requirements, a wide variety of seeding particles is available for PIV experiments. Tables 3 and 4 review the types of particles which have been used in recent years in gases and liquids respectively. Within the space limitations of a tabular summary only the particle material (refractive index m and density ρ, not accounting for coagulation effects with solid particles), the particle diameter d_p, the type of laser and the width w and the thickness t of the light sheet are included as prominent experimental features. The light sheet dimensions and the laser characteristics together indicate qualitatively the interaction between the choice of particle diameter and the scattered light intensity. CW lasers, such as Ar ion lasers (wavelength 488 or 514.5 nm), and pulsed lasers, such as frequency-doubled Nd:YAG (wavelength 532 nm), ruby (wavelength 694 nm) and copper vapour (wavelength 511 nm) lasers, must be gated for PIV applications.

In table 3 it is clear that in almost all cases a particle diameter near or below 1 μm has been used for seeding in gas flows, which is consistent with the requirements of section 3 for particles with a high density ratio s as summarized in the examples of table 2. A consequence of the small particle size is the need for a high laser pulse energy, in most cases 100 mJ or more. Ceramic materials such as Al_2O_3, TiO_2 and ZrO_2 are favoured for seeding flames and high-temperature flows and also offer the advantage of a high refractive index, although their dispersion in a gas flow (like that of other powders) can be difficult (section 5). Slightly larger seeding particles were used in the combustor experiments of Anderson *et al* (1996), but according to table 2 these particles should have tracked turbulence frequencies up to nearly 1 kHz. In their investigations of the flow around wind turbine rotors by particle image velocimetry, Grant *et al* (1994) undertook experiments in open terrain. The seeding particles were undoubtedly too large for precise tracking, but this was presumably less critical than the acquisition of sufficiently strong signals under unfavourable conditions.

The examples of table 4 show that much larger seeding particles have frequently been used in liquid flows, permitting PIV experiments with gated argon ion lasers rather than pulsed lasers. The particles in these experiments were chosen to have nearly neutral density ($\rho \approx 1000$ kg m^{-3}) for experiments in water, so that adequate tracking responses could still be expected. In the first two cases cited in the table (Longmire and Alahyari 1994, Liu *et al* 1991) ceramic seeding particles were used, so that with density ratios $s = 3.5$–4 rather small particles and pulsed lasers became necessary. Dieter *et al* (1994), on the other hand, used hydrogen bubbles with a very low density ratio leading to possible buoyancy effects. Graham and Soria (1994) used hollow glass spheres as scatterers with a density ratio slightly below unity and good tracking capability in water. Favourable flow and light scattering characteristics are also offered by hollow polymer microballoons (Sankar *et al* (1992), diameter 40–50 μm) and by porous or hollow SiO_2 microballoons (Ikeda *et al* (1992), density $\rho = 200$–800 kg m^{-3} and refractive index $m = 1.70$).

5. The generation and seeding of scattering particles

5.1. The generation of scattering particles

The generation of scattering particles for liquid flows is almost trivial, since it is seldom necessary to do more than mix particles in powder form or as a suspension into the flow. The work of Dieter *et al* (1994) is unusual in this respect; electrolysis was used to generate fine gas bubbles as tracer particles in water.

Gas flows can be seeded either with liquid droplets or with solid particles. For droplets the techniques of atomization and condensation are feasible, whereas for solid particles atomization (of solutions or suspensions of the particles) and fluidization come into consideration. Generators should ideally produce particles with a nearly monodisperse size distribution, at a high enough rate to achieve adequate spatial resolution of PIV in the flow field. According to the recommendations of Keane and Adrian (1990) about 15 particles are required per interrogation volume; the number of seeding particles must thus be increased at higher flow velocities.

Seeding with liquid droplets offers the advantage of a steadier production rate than is normally feasible with solid particles. Their inherently spherical shape is also advantageous for assessing tracking behaviour and scattering characteristics; moreover, information on the refractive index is more readily available for liquids than it is for many solids. Seeding droplets depositing on windows in internal flows can form non-uniform liquid films, leading to beam distortion by refraction; the consequent defocusing or deflection may be serious enough to cause temporary or permanent loss of signals.

Solid particles are preferable when high particle concentrations are necessary, but the resulting tendency for increased coagulation as a result of electrostatic forces or moisture must be recognized. In flames and high-temperature flows non-volatile solid particles are essential. Solid particle deposits on windows mainly cause beam attenuation with less serious consequences than those encountered with liquid deposits.

5.1.1. The generation of droplets by condensation. In its simplest form a condensation aerosol is an oil fog, as used for PIV by Stewart *et al* (1996). The oil is evaporated by a heater and the vapour condenses to fine droplets in the gas flow. Such seeding, however, is difficult to regulate, so the delivery rate tends to be unsteady and the droplet size distribution rather wide. If, on the other hand, the condensation process is allowed to proceed at a uniform temperature onto seed nuclei introduced at a controlled concentration, as in the classical generator of Sinclair and LaMer (Green and Lane 1964), a nearly monodisperse droplet size distribution can be achieved. The attainable concentration, however, is very low. (This compromise between quality and concentration of the aerosol applies, indeed, in varying degree to all types of generator.) Meyers and Feller (1975) did develop a condensation aerosol generator for seeding a high-speed air flow for LDA measurements, but in general this type of generator has not found favour, probably because of the complexity necessary for satisfactory results.

5.1.2. The generation of droplets by atomization. Of the various types of atomizer available, the nebulizer (also known as twin-fluid or air-assist atomizer) is most suitable to generate particles of sufficiently small size for PIV. Liquid is drawn from a supply reservoir by the low static pressure of an entraining gas jet and forms a thin liquid film which is sheared and ruptured by the high velocity gas flow and then disintegrates into individual droplets. This process leads to the production of a polydisperse spray, so the use of an impactor to remove the larger droplets is advantageous. Alternatively these can be removed by collision with the container wall of the atomizer, whence they drain as a wall film back into the reservoir. Particle concentrations as high as about 1–10 mm^{-3} (10^9–10^{10} m^{-3}) can be achieved.

A simple nebulizer suitable for seeding gas flows at low pressure is the Inspiron model 002305-A (Intertech Resources Inc, USA). More sophisticated is the Six-Jet Atomizer model 9306 available from TSI Inc, St Paul, USA. By varying the number of atomizers in parallel, the seeding flow rate can be adjusted to suit the gas flow.

A robust design which permits flexible and readily controlled operation is the Laskin atomizer (figure 5). Detailed information on the construction and performance, as well as variations in design, was given by Echols and Young (1963). Air or gas is blown through four holes in a tube into the liquid in the reservoir. These four jets then draw liquid up through vertical holes in the ring, to produce air bubbles containing finely atomized droplets. As the bubbles rise to the liquid surface, the droplets are released into the gas stream. An impactor is necessary to remove larger droplets from the polydisperse spray. The rate of generation can be increased by using multiple atomizer nozzles in the same tank. It is also possible with this type of generator to deliver seeding particles into flows under pressure, for example with a back pressure of 4 bar on the generator.

Details of an alternative atomizer design with some similarities to the Laskin nozzle are shown in figure 6. Compressed air blown sideways through three 1 mm holes in the nozzle sucks liquid up from the reservoir through vertical holes and atomizes it. The lateral holes are located above the liquid level and larger droplets in the spray are rejected after impact against the ring surrounding the nozzle head. A second impactor is used downstream to achieve a finer spray. By using a solution of oil (such as paraffin) in a volatile solvent, oil droplets can be generated that are smaller than the originally atomized droplets.

5.1.3. The generation of solid particles by atomization. The atomization of solutions or suspensions with a volatile solvent or suspending liquid is one possibility for seeding with solid particles. The advantage of a steady concentration can thus be maintained. The atomizer designs of section 5.1.2 are suitable for this purpose.

Atomization of suspensions lends itself particularly to seeding solid particles of uniform size, starting from a

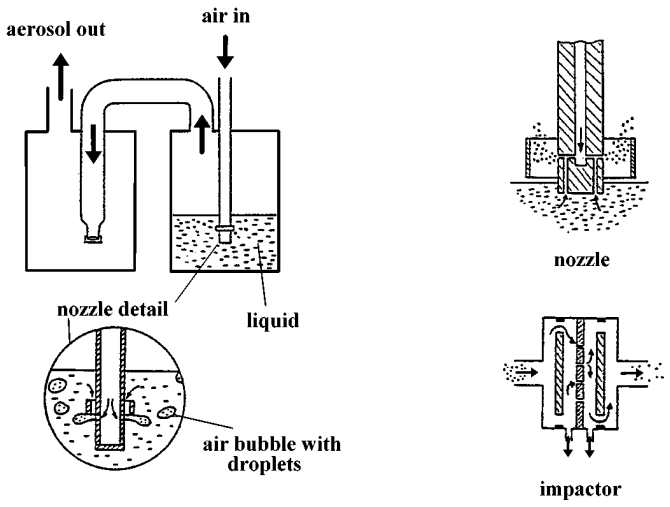

Figure 5. A Laskin nozzle.

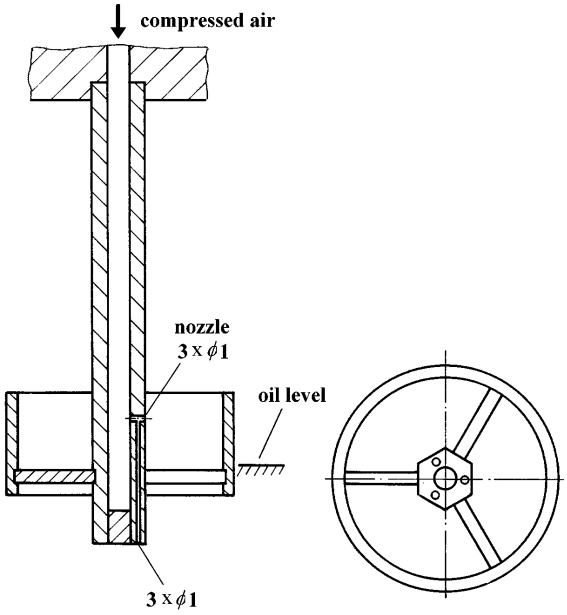

Figure 6. An alternative atomizer design.

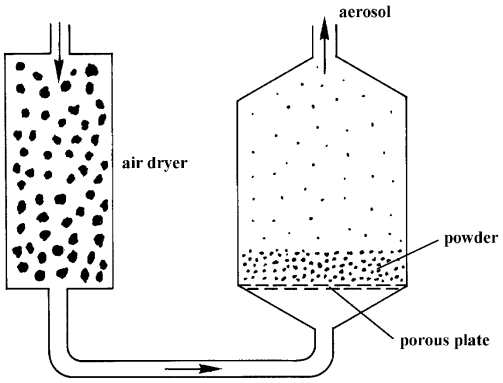

Figure 7. A fluidized bed aerosol generator.

suspension of (expensive) monodisperse particles, such as polystyrene latex in water suspension. The droplets first formed by atomization are polydisperse, but the aerosol of solid particles will be monodisperse after evaporation of the suspending liquid if no droplet contains more than one solid particle. This condition can be attained by using a dilute suspension, but the aerosol concentration is then low, since many droplets formed are empty. Paone *et al* (1996) have used this method to disperse TiO_2 and ZrO_2 particles from a 5% ethyl alcohol suspension for PIV in flames.

Aerosols of solid particles formed from solution are normally polydisperse, because the particle diameter depends on the initial droplet diameter and the concentration of the solution. With a low enough concentration solid particles well below 1 μm in size can be produced.

5.1.4. The generation of solid particles from powders. Solid particles for gas flows are mostly generated in fluidized beds of various designs, for example figures 7 and 8. A powder of submicrometre particles is suspended in the bed and the aerosol is drawn from the top. The particles dispersed into the gas stream are normally several times larger than the nominal particle size of the powder in the bed because of coagulation which depends on the humidity of the gas and the moisture content of the powder and on the rate of flow through the bed. Smooth, hard, dry particles disperse more easily than do rough, soft, moist particles, although extreme dryness can restrict the dispersion because of electrostatic forces. Coagulation tends to reduce the number concentration N of the smaller particles in favour of the larger particles. The rate of coagulation varies as N^2, so the effect is important in the generator and the seeding delivery tube, before the concentration is reduced

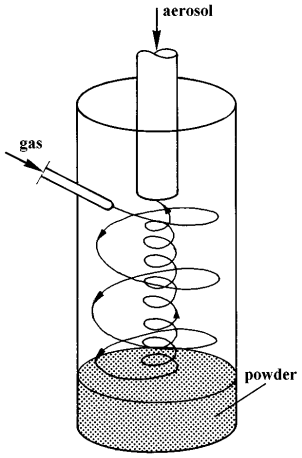

Figure 8. A cyclone aerosol generator.

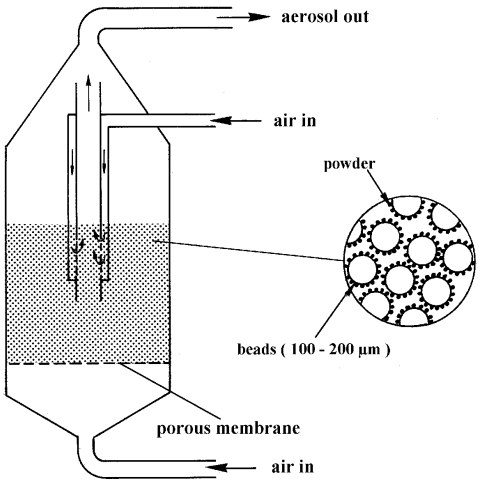

Figure 9. A 'two-phase' fluidized bed.

by dilution in the flow. Aggregation tends to increase as the flow through the bed is increased, so that the bed density becomes non-uniform and is disturbed by bubbles or slugs of air, leading to an erratic rate of generation.

To improve the stability of the particle generation from a fluidized bed, Glass and Kennedy (1977) used an additional cyclone to obtain 0.1–1 μm Al_2O_3 particles (figure 8). For particle concentrations above 10^9 m^{-3}, concentration fluctuations were greatly reduced. This generator design was adopted for PIV experiments, for example, by Anderson *et al* (1996).

In an effort to obtain steadier distributions of concentration and particle size than is possible with conventional fluidized beds, two-phase beds have been developed (Willeke *et al* 1974, Guichard 1976). The bed (figure 9) contains a mixture of beads (nickel, bronze or glass, diameter 100–200 μm) and the powder to be dispersed. The suspended powder particles are much smaller than the beads and can move freely in the volume between the beads without forming gas bubbles. The continuous friction between the beads reduces the aggregation of the powder particles. The upwards gas velocity is set between the gravitational settling velocities of the particles and the beads, so that the beads are fluidized but not entrained. The powder particles are elutriated from the bed by rising gas bubbles which burst at the surface of the bed, releasing the particles. A generator of essentially this type was previously offered commercially for LDA and PIV experiments by TSI Inc, St Paul, USA, but is now no longer in production. The design and operating characteristics of such a generator, although it was not intended for PIV experiments, were described by Boucher and Lua (1982).

The simple fluidized bed or variants thereof has been found to be more practical than, for example, the complicated spark discharge generator described by Altgeld *et al* (1980). An ultrasonic disperser is another means of introducing larger seeding particles into an air stream and has been used by Schmidt and Löffler (1993) with 30 μm glass particles for PIV experiments.

5.2. The seeding of scattering particles

5.2.1. Seeding in liquid flows. Investigations with PIV in liquid flows are almost always undertaken in closed-circuit test loops. It is, therefore, possible to introduce a concentrated suspension of seeding particles into the flow before starting the measurements and allow the particles to mix thoroughly and uniformly in the circulating flow. Dilutions up to 1:50 000 are feasible. Preferentially, monodisperse suspensions, such as latex particles, should be used, but these are mostly too expensive to be used in large quantities.

5.2.2. Seeding in gas flows. Seeding particles should be introduced into the flow in sufficient and stable concentration, with a spatially uniform distribution, while minimizing coagulation and deposition of particles on windows. Frequently a choice must be made between global and local seeding.

Global seeding, with the particles introduced into the flow well upstream of the region of measurement, is preferable to ensure that seeding occurs everywhere in this region, so that velocities over the whole flow field of a PIV experiment are represented. As a means of obtaining a spatially homogeneous, though necessarily rather low, seeding concentration in a closed-circuit wind tunnel, Smith *et al* (1992) introduced the particles downstream of the test section and allowed them to recirculate through the blower. Possibilities for varying the seeding concentration in a closed-circuit tunnel include running the seeding generator intermittently or allowing the tunnel to run full and then switching off the generator, so that the concentration falls to a level suitable for PIV measurements. These methods are, of course, only feasible if the maximum achievable seeding concentration exceeds requirements. In most larger wind tunnels seeding the entire flow is not possible because of the limited production rate of aerosol generators.

If only a restricted portion of the flow field is of interest, it may be acceptable to seed only the stream tube passing through the observation area and so attain a higher

concentration. It must, however, still be the objective of local seeding to seed this part of the flow uniformly. Moreover, flow disturbance must be avoided by mounting the seeding probe sufficiently far upstream of the zone of measurement, or better by introducing the seeding in a settling chamber. The probe position will be a compromise, because turbulent diffusion will reduce the concentration with increasing distance downstream from the probe.

Seeding in swirling flows poses further problems. When seeding locally it is difficult to locate the stream tube which exactly coincides with the vortex core. Furthermore, the density in the core is reduced, leading to a lower seeding concentration. The problem of radial acceleration of particles out of the vortex core under the influence of the centrifugal force has been referred to in section 3.1.

5.2.3. High-speed flows. High speeds, particularly transonic and supersonic flows, pose particular difficulties with respect to the generation and seeding of particles. The Laskin nozzle has been used with great success to generate olive oil droplets as scatterers for PIV studies in transonic flows (Höcker and Kompenhans 1991, Raffel *et al* 1996). With several Laskin nozzles in parallel, seeding densities of up to four particles mm^{-3} were obtainable, corresponding to about 30 particles per interrogation volume, well in excess of the minimum specified by Keane and Adrian (1990). The aerodynamic diameter was determined experimentally to be about 1 μm, ensuring that there would be an adequate aerodynamic response of the droplets to velocity gradients in the flow. In this respect it should be borne in mind that the resolution of the PIV velocity measurement in such applications is ultimately limited not by the aerodynamic response of the particle but by the spatial averaging of the PIV recording within each interrogation volume. Since these volumes have dimensions of several millimetres, a shock (of width several micrometres) cannot be resolved. A possibly more severe criterion for the particle size according to the considerations in section 3.3 is, therefore, unnecessary.

In supersonic flow Lepicovsky and Bruckner (1996) reported a particular difficulty when atomizing an alcohol suspension of polystyrene latex particles (PSL, 1.1 μm diameter). Following atomization the alcohol evaporated, leaving the desired PSL seeds, but after expansion and cooling of the air in the supersonic wind tunnel it condensed again, forming droplets which were too large to follow the flow.

6. Summary

The problems confronted when seeding a flow for PIV experiments are similar to those for LDA; the extensive literature and experience from LDA can, therefore, provide assistance. Criteria for the maximum size of seeding particles to ensure acceptable flow tracking demand particle diameters of about 1 μm or smaller for most seeding materials in typical turbulent or high speed gas flows. A larger maximum particle size and hence a larger scattering cross section is feasible by using hollow or porous particles with a lower density ratio. The case of unity particle–fluid density ratio, namely perfect tracking, can be approximated in liquid flows.

For high quality PIV records a scattering particle concentration of about 15 particles per interrogation volume is necessary. The size of the interrogation volume depends in turn on the dimensions of the test section, but for many laboratory applications this condition corresponds to a concentration of 10^8–10^{10} m^{-3}. Suitable generators to satisfy the particle size and concentration requirements in gas flows are twin-fluid atomizers (for droplets or solid particles in liquid suspension) and fluidized beds (for solid particles). Ideally the scattering particles should be distributed uniformly in the flow, but, with large volume flow rates, requirements for globally uniform seeding may exceed the particle generation capacity. If local seeding is adopted, uniformity of seeding must be achieved in the region of investigation.

References

Altgeld H, Schnettler A and Stehmeier D 1980 Spark discharge particle generator for laser Doppler anemometry *J. Phys. E: Sci. Instrum.* **13** 437–41

Anderson D J, Greated C A, Jones J D C, Nimmo G and Wiseall S 1996 Fibre optic PIV studies in an industrial combustor *Proc. 8th Int. Symp. on Applications of Laser Techniques to Fluid Mechanics, Lisbon* paper 18.4

Basset A B 1888 *Treatise on Hydrodynamics* vol II (London: Deighton, Bell & Co)

Boucher R F and Lua A C 1982 A stable, high concentration, dry aerosol generator *J. Aerosol Sci.* **13** 499–511

Chao B T 1964 Turbulent transport behaviour of small particles in a turbulent fluid *Österreichisches Ingenieur-Archiv* **18** 7

Dieter J, Bremeyer R, Hering F and Jähne B 1994 Flow measurements close to the free air/sea interface *Proc. 7th Int. Symp. on Applications of Laser Techniques to Fluid Mechanics, Lisbon* paper 22.2

Draad A A and Westerweel J 1996 Measurement of temporal and spatial evolution of transitional pipe flow with PIV *Proc. 8th Int. Symp. on Applications of Laser Techniques to Fluid Mechanics, Lisbon* paper 29.3

Dring R P 1982 Sizing criteria for laser anemometry particles *Trans. ASME, J. Fluids Eng.* **104** 15–17

Durst F, Melling A and Whitelaw J H 1981 *Principles and Practice of Laser-Doppler Anemometry* (London: Academic)

Echols W H and Young J A 1963 Studies of air-operated aerosol generators, NRL report 5929, US Naval Research Laboratory, Washington

Fischer M 1994 Comparison of PIV with hot-wire measurements and calculations obtained for instabilities in a flat plate boundary layer *Proc. 7th Int. Symp. on Applications of Laser Techniques to Fluid Mechanics, Lisbon* paper 37.4

Gallagher M W and McEwan I K 1996 Insights into grain entrainment using particle image velocimetry *Proc. 8th Int. Symp. on Applications of Laser Techniques to Fluid Mechanics, Lisbon* paper 38.2

Glass M and Kennedy I M 1977 An improved seeding method for high temperature laser Doppler velocimetry *Combustion Flame* **49** 155–62

Graham L J W and Soria J 1994 A study of an inclined cylinder wake using digital particle image velocimetry *Proc. 7th Int. Symp. on Applications of Laser Techniques to Fluid Mechanics, Lisbon* paper 37.2

Grant I 1997 Particle image velocimetry: a review *Proc. Inst. Mech. Eng.* C **211** 55–76

Grant I, Owens E, Stewart J N and Aroussi A 1992 Particle image velocimetry measurements of propellor-hull wake interaction behind a model ship *Proc. 6th Int. Symp. on Applications of Laser Techniques to Fluid Mechanics, Lisbon* paper 39.3

Grant I, Smith G H, Infield D, Wang X, Zhao Y and Fu S 1994 Measurements of the flow around wind turbine rotors by particle image velocimetry *Proc. 7th Int. Symp. on Applications of Laser Techniques to Fluid Mechanics, Lisbon* paper 10.5

Grant I and Wang X 1994 Directionally unambiguous, digital particle image velocimetry studies using an image intensifier camera *Exp. Fluids* **18** 358–62

Green H L and Lane W R 1964 *Particulate Clouds: Dusts, Smokes and Mists* 2nd edn (London: E & F N Spon)

Guichard J C 1976 Aerosol generation using fluidized beds *Fine Particles* ed B Y H Liu (New York: Academic) pp 173–93

Haertig J 1976 Introductory lecture on particle behaviour *ISL/AGARD Workshop on Laser Anemometry (Institut Saint Louis)* report R 117/76

Hart D P 1996 Sparse array image correlation *Proc. 8th Int. Symp. on Applications of Laser Techniques to Fluid Mechanics, Lisbon* paper 21.1

Hassan Y A, Martinez R S, Philip O G and Schmidl W D 1994 Flow measurement of a two-phase fluid around cylinders in a channel using particle image velocimetry *Proc. 7th Int. Symp. on Applications of Laser Techniques to Fluid Mechanics, Lisbon* paper 37.5

Hjemfelt A T and Mockros L F 1996 Motion of discrete particles in a turbulent fluid *Appl. Sci. Res.* **16** 149

Höcker R and Kompenhans J 1991 Application of particle image velocimetry to transonic flows *Applications of Laser Techniques to Fluid Mechanics (Proc. 5th Int. Symp., Lisbon 1990)* (Berlin: Springer) pp 415–34

Ikeda Y, Nishigaki M, Ippommatsu M, Hosokawa S and Nakajima T 1992 Optimum seeding particles for successful LDV experiments *Proc. 6th Int. Symp. on Applications of Laser Techniques to Fluid Mechanics, Lisbon* paper 32.2

Jakobsen M L, McCluskey D R, Easson W J, Glass D H and Greated C A 1994 Pneumatic particle conveyance in pipe bend: simultaneous two-phase PIV measurements of the slip velocity between the air and the particle phases *Proc. 7th Int. Symp. on Applications of Laser Techniques to Fluid Mechanics, Lisbon* paper 31.4

Johari H, Dabiri D, Weigand A and Gharib M 1996 On the relationship between the formation number and passive scalar pinch-off in starting jets *Proc. 8th Int. Symp. on Applications of Laser Techniques to Fluid Mechanics, Lisbon* paper 30.1

Keane R D and Adrian R J 1990 Optimization of particle image velocimeters. Part I: double pulsed systems *Meas. Sci. Technol.* **1** 1202–15

Khoo B C, Chew T C, Heng P S and Kong H K 1992 Turbulence characterisation of a confined jet using PIV *Exp. Fluids* **13** 350–6

Krothapalli A, Wishart D P and Lourenco L M 1994 Near field structure of a supersonic jet: 'on-line' PIV study *Proc. 7th Int. Symp. on Applications of Laser Techniques to Fluid Mechanics, Lisbon* paper 26.5

Lepicovsky J and Bruckner R J 1996 Seeding for laser velocimetry in confined supersonic flows with shocks *Proc. 8th Int. Symp. on Applications of Laser Techniques to Fluid Mechanics, Lisbon* paper 15.1

Liu Z-C, Landreth C C, Adrian R J and Hanratty H J 1991 High resolution measurement of turbulent structure in a channel with particle image velocimetry *Exp. Fluids* **10** 301–12

Longmire E K and Alahyari A 1994 PIV measurements in simulated microbursts *Proc. 7th Int. Symp. on Applications of Laser Techniques to Fluid Mechanics, Lisbon* paper 37.1

Magness C, Robinson O and Rockwell D 1993 Laser-scanning particle image velocimetry applied to a delta wing in transient maneuver *Exp. Fluids* **15** 159–67

McCluskey D R, Laursen T S, Rasmussen J J and Stenum B 1995 Evolution of vortical flow fields measured by real time PIV system *Laser Anemometry* (New York: ASME) pp 313–18

——1996 Damping of a vortex ring in a stratified fluid *Proc. 8th Int. Symp. on Applications of Laser Techniques to Fluid Mechanics, Lisbon* paper 35.4

Mei R 1996 Velocity fidelity of flow tracer particles *Exp. Fluids* **22** 1–13

Melling A and Whitelaw J H 1973 Seeding of gas flows for laser anemometry *DISA Information* **15** 5–14

Meyers J F and Feller W V 1975 Development of a controllable particle generator for LV seeding in hypersonic wind tunnels *Minnesota Symp. on Laser Anemometry* p 345

Mengel F and Mørck T 1993 Prediction of PIV recording performance *Proc. SPIE* **2052** 331–8

Muniz L, Martinez R E and Mungal M G 1996 Applications of PIV to turbulent reacting flows *Proc. 8th Int. Symp. on Applications of Laser Techniques to Fluid Mechanics, Lisbon* paper 3.3

Paone N, Revel G M and Nino E 1996 Velocity measurement in high turbulent premixed flames by a PIV measurement system *Proc. 8th Int. Symp. on Applications of Laser Techniques to Fluid Mechanics, Lisbon* paper 3.4

Raffel M, Höfer H, Kost F, Willert C and Kompenhans J 1996 Experimental aspects of PIV measurements of transonic flow fields at a trailing edge model of a turbine blade *Proc. 8th Int. Symp. on Applications of Laser Techniques to Fluid Mechanics, Lisbon* paper 28.1

Reuss D L, Adrian R J, Landreth C C, French D T and Fansler T D 1989 Instantaneous planar measurements of velocity and large-scale vorticity and strain rate in an engine using particle-image velocimetry, SAE paper 890616

Roth G, Hart D and Katz J 1995 Feasibility of using the L64720 video motion estimation processor (MEP) to increase efficiency of velocity map generation for particle image velocimetry (PIV) *Laser Anemometry* (New York: ASME) pp 387–93

Saffman P G 1965 The lift on a small sphere in a slow shear flow *J. Fluid Mech.* **22** 385–400

Sankar S V, Kamemoto D Y and Bachalo W D 1992 An evaluation on the use of large, hollow micro-balloons as LDV seed particles *Proc. 6th Int. Symp. on Applications of Laser Techniques to Fluid Mechanics, Lisbon* paper 32.3

Schmidt M and Löffler F 1993 Experimental investigations on two-phase flow past a sphere using digital particle-image-velocimetry *Exp. Fluids* **14** 296–304

Smith G H, Grant I, Liu A, Infield D and Eich T 1992 A wind tunnel examination of vortices shed from a wind generator using particle image velocimetry *Proc. 6th Int. Symp. on Applications of Laser Techniques to Fluid Mechanics, Lisbon* paper 13.5

Stewart J N, Wang Q, Moseley R P, Bearman P W and Harvey J K 1996 Measurement of vortical flows in a low speed wind tunnel using particle image velocimetry *Proc. 8th Int. Symp. on Applications of Laser Techniques to Fluid Mechanics, Lisbon* paper 18.5

Westergaard C H, Buchhave P and Sorensen J N 1993 PIV measurements of turbulent and chaotic structures in a rotating flow using an optical correlator *Laser Techniques and Applications in Fluid Mechanics (Proc. 6th Int. Symp., Lisbon 1992)* (Berlin: Springer) pp 243–56

Westerweel J, Adrian R J, Eggels J G M and Nieuwstadt F T M 1993 Measurements with particle image velocimetry on fully developed turbulent pipe flow at low Reynolds number *Laser Techniques and Applications in Fluid Mechanics (Proc. 6th Int. Symp., Lisbon 1992)* (Berlin: Springer) pp 285–310

Willeke K, Lo C S K and Whitby K 1974 Dispersion characteristics of a fluidized bed *Aerosol Sci.* **5** 449–55

Willert C E and Gharib M 1991 Digital particle image velocimetry *Exp. Fluids* **10** 181–93

Zhang J, Tao B and Katz J 1996 Three dimensional velocity measurements using hybrid HPIV *Proc. 8th Int. Symp. on Applications of Laser Techniques to Fluid Mechanics, Lisbon* paper 4.3